

## 钒氮共掺杂多孔碳催化剂上苄胺氧化偶联合成亚胺

吴晓雪 齐妍妍 王盈懿 王丽 涂高美 傅仰河 陈德利 朱伟东 张富民\*

(先进催化材料教育部重点实验室,浙江师范大学物理化学研究所,金华 321004)

**摘要:**本工作以生物质壳聚糖作为牺牲模板,乙酰丙酮钒为金属钒源, $ZnCl_2$ 为造孔剂,采用高温热解结合酸洗的策略制备出一种钒氮共掺杂多孔碳(V-N-C)催化剂。表征结果表明,V-N-C催化剂的比表面积高达 $1\ 470\ m^2\cdot g^{-1}$ ,孔容为 $1.06\ cm^3\cdot g^{-1}$ ,质量分数为0.19%的钒物种可能以单原子 $VN_x$ 形式高度分散在载体上。在苄胺氧化偶联合成亚胺的反应中,V-N-C表现出高催化性能,底物苄胺的转化率和产物亚胺的选择性均为99%,性能明显优于均相 $VO(acac)_2$ 和多相 $V_2O_5$ 催化剂。此外V-N-C催化剂连续重复使用9次也未出现任何活性衰减的问题,且对一系列含有不同官能团的底物也具有优良的普适性。机理研究表明,苄胺和氧气首先分别在催化剂 $VN_x$ 和缺陷位点活化成苄基亚胺和 $H_2O_2$ 中间体,然后苄基亚胺与苄胺缩合脱 $NH_3$ 生成目标产物亚胺。

**关键词:**选择性催化氧化;多相催化;钒氮共掺杂多孔碳;氧化偶联

中图分类号:0614.51; 0643.36 文献标识码:A 文章编号:1001-4861(2022)06-1049-10

DOI:10.11862/CJIC.2022.112

## Synthesis of Amines by Oxidative Coupling of Benzylamine over a Vanadium-Nitrogen Co-doped Porous Carbon Catalyst

WU Xiao-Xue QI Yan-Yan WANG Ying-Yi WANG Li TU Gao-Mei

FU Yang-He CHEN De-Li ZHU Wei-Dong ZHANG Fu-Min\*

(Key Laboratory of the Ministry of Education for Advanced Catalysis Materials,

Institute of Physical Chemistry, Zhejiang Normal University, Jinhua, Zhejiang 321004, China)

**Abstract:** Synthesis of imine compounds via benzylamine oxidative coupling has become one of the most ideal methods due to its high atom economy and environmental friendliness. The key is to develop high-performance non-noble metal-based heterogeneous catalysts. In this work, a vanadium-nitrogen co-doped porous carbon (V-N-C) catalyst was prepared via high-temperature pyrolysis (900 °C for 2 h in an inert atmosphere) combined with acid-leaching (1 mol·L<sup>-1</sup> HCl solution at 120 °C for 12 h) approach by using biomass chitosan as the sacrificial template, vanadium acetylacetone as the source of metal vanadium, and  $ZnCl_2$  as the pore-forming agent. Various characterization techniques including a high-angle annular dark-field scanning transmission electron microscopy (HAADF-STEM) investigation were used to analyze the composition, structure, vanadium species size, content, and other physical and chemical properties of the catalyst, and its catalytic performance was evaluated in the oxidative coupling reaction of benzylamine. The characterization results showed that the specific surface area of the V-N-C catalyst was as high as  $1\ 470\ m^2\cdot g^{-1}$ , the pore volume was  $1.06\ cm^3\cdot g^{-1}$ , and the mass fraction of the vanadium species was 0.19% that were highly dispersed on the support likely in the form of single atoms ( $VN_x$ ). In the oxidative self-coupling reaction of benzylamine to the imine (reaction conditions: toluene as solvent, 110 °C,  $1.01\times 10^5\ Pa\ O_2$ , 12 h), the developed V-N-C exhibited excellent activity (99%), exclusive selectivity (99%), outperforming the homogeneous  $VO(acac)_2$  and heterogeneous  $V_2O_5$  catalysts. Moreover, V-N-C was repeatedly used 9 times without any decay

收稿日期:2022-01-12。收修改稿日期:2022-04-14。

国家自然科学基金(No.21576243)资助。

\*通信联系人。E-mail:zhangfumin@zjnu.edu.cn

in reactivity and stability. Furthermore, V-N-C presented excellent universality for a series of substrates containing different functional groups. Mechanism studies indicated that the reaction steps were involved in the initial formation of benzylimine and H<sub>2</sub>O<sub>2</sub> intermediates by activating benzylamine and oxygen molecules, respectively, on the VN<sub>x</sub> and defect sites of V-N-C, then benzylimine and benzylamine condensed to release an NH<sub>3</sub> molecule to generate the target product imine.

**Keywords:** selective catalytic oxidation; heterogeneous catalysis; vanadium-nitrogen co-doped porous carbon; oxidative coupling

## 0 引言

亚胺是含有C=N双键结构的杂环化合物，在环化、氧化还原、加成和缩合等有机反应中作为常见的中间体<sup>[1]</sup>。含有杂原子(氧、硫、磷等)的亚胺配体可以与金属离子形成金属配合物，应用于一系列具有生物和药理活性的化合物、杂环或者天然产物的合成<sup>[2-4]</sup>。传统亚胺主要是通过在均相路易斯酸催化剂的作用下进行伯胺和羰基化合物的缩合反应来获得<sup>[5-6]</sup>，其缺点是反应过程需要加入脱水剂和使用不稳定的醛基原料来提高反应效率，导致底物利用率低、操作复杂以及对环境造成污染等<sup>[7]</sup>。在有氧化剂的条件下，通过胺的氧化偶联合成亚胺是一条绿色的路线。近年来已有许多催化体系被报道，包括贵金属催化剂<sup>[8-11]</sup>、光催化剂<sup>[12-14]</sup>等，但上述大多数反应存在产率或选择性较低、反应条件相对苛刻、底物适用范围受限等不足。因此，从绿色和可持续的化学观出发，亟待开发一种新型绿色高效的过渡金属催化剂。

过渡金属(M)与杂原子氮共掺杂多孔碳(M-N-C)材料是一类具有广阔应用前景的催化剂，其多孔碳骨架结构有利于反应物和产物的吸附/扩散，从而提高催化活性<sup>[15-18]</sup>。而杂原子N的孤对电子可以捕获金属中心，形成稳定的金属活性位点，因而可高效催化多种有机反应<sup>[19-20]</sup>。壳聚糖作为可再生生物质，其结构中含有氨基和羟基功能性基团，具有较强的配位能力，可有效螯合金属离子。壳聚糖-金属配合物衍生材料不仅部分继承载体材料的特点，还有望保留金属中心高度分散的特性，是制备过渡金属基与氮共掺杂碳材料的理想前驱体<sup>[21-23]</sup>。此外，在壳聚糖碳化处理过程中，引入造孔剂ZnCl<sub>2</sub>，既可有效降低焦油的产生<sup>[10]</sup>，还可以促进C、H、O间的交联反应，有助于形成多孔结构，增大材料的比表面积<sup>[24]</sup>，进而提高催化活性和选择性。

以生物质壳聚糖为牺牲模板，VO(acac)<sub>2</sub>为金属钒源，ZnCl<sub>2</sub>为活化造孔剂，采用碳热处理结合酸洗

的策略合成出一种高比表面积的钒氮共掺杂多孔碳(V-N-C)催化剂。考察了该催化剂在以O<sub>2</sub>为氧化剂、甲苯为溶剂的苄胺及其衍生物氧化偶联反应中的催化性能，并初步推测了可能的反应机理。

## 1 实验部分

### 1.1 主要试剂

壳聚糖于国药集团化学试剂公司购买；乙酰丙酮钒、氯化锌于上海迈瑞尔化学技术有限公司购买；甲苯、N,N-二甲基甲酰胺、苄胺、对甲氧基苄胺、对甲基苄胺、2-甲基苄胺、3-甲基苄胺、对叔丁基苄胺、4-氟苄胺、4-氯苄胺、4-溴苄胺、4-三氟甲基苄胺、苯胺、3-吡啶甲胺、噻吩2-甲胺、糠胺、正己胺、1,2,3,4-四氢喹啉、二苄基胺、环己胺于上海阿拉丁公司购买；邻氨基苯硫酚、2-氨基苯硫酚、对甲氧基苯胺、对氯苯胺、对甲基苯胺购自北京伊诺凯公司。以上试剂均为分析纯，高纯N<sub>2</sub>(99.999%)于上海大通气体有限公司购买。

### 1.2 催化剂表征

采用X射线衍射仪(XRD, D8 Adance型)分析了催化剂的晶体结构，表征条件：工作电压为40 kV，电流40 mA，辐射源为Cu靶K $\alpha$ 射线，波长为0.154 2 nm，2θ范围为2°~80°。通过拉曼光谱仪(Renishaw RM 10000, 532 nm)对样品的石墨化程度和缺陷程度进行了分析。采用配有E-1030喷金装置的扫描电子显微镜(SEM, S-4800型, 5 kV)和透射电子显微镜(TEM, JEM-2100F, 200 kV)对样品的形貌进行了表征。利用球差校正的高角度环形暗场扫描透射电子显微镜(HAADF-STEM, FEI Themis Z)探究催化剂中金属物种的尺寸及分散情况。采用物理吸附仪(Micromeritics ASAP 2020型)测定-196 °C时催化剂的氮气吸附-脱附等温线。使用X射线光电子能谱仪(XPS, Thermo ESCALAB 250XI)获得样品元素价态，表征条件：辐射源为Al K $\alpha$ 射线(1 486.6 eV)，系统真空度低于1.0×10<sup>-7</sup> Pa。采用电感耦合等离子体

发射光谱仪(ICP-AES, iCAP 7400, Thermo, USA)测定金属含量。

### 1.3 催化剂制备

V-N-C催化剂的制备:将2 g壳聚糖溶解在120 mL 0.5%乙酸溶液中,再加入6.5 g氯化锌和20 mg乙酰丙酮钒,搅拌混匀,80 °C水浴条件下回流反应8 h。然后将样品转入冷冻干燥机中进行干燥处理12 h。将干燥的样品研磨后置于刚玉舟中,放于管式炉,在N<sub>2</sub>气氛下,以3 °C·min<sup>-1</sup>升温到900 °C,进行碳

化处理2 h。随后将样品转移到装有50 mL 1 mol·L<sup>-1</sup> HCl溶液的圆底烧瓶中,120 °C油浴条件下酸洗12 h,去除不稳定的金属或者金属氧化物,冷却后抽滤洗涤,放入真空烘箱120 °C干燥12 h,可得黑色固体,将其命名为V-N-C。制备示意图如图1所示。氮共掺杂多孔碳材料(N-C)的制备:采用上述相似的方法,只是在合成中不添加金属钒源,制得黑色固体为N-C。

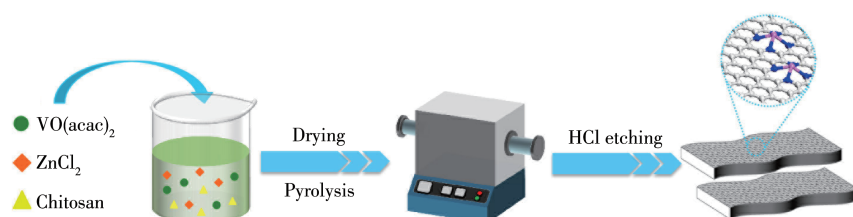


图1 V-N-C催化剂的合成示意图

Fig.1 Schematic illustration of the synthesis process of V-N-C catalyst

### 1.4 苄胺氧化偶联反应

称取30 mg V-N-C催化剂,量取3 mL甲苯和0.5 mmol苄胺,并依次加入到10 mL的Schlenk管中并连通氧气袋。在反应前,先用氧气置换试管内的空气(重复3次),随后将反应管置于110 °C的油浴锅中开始计时进行反应。定时取样,液相混合物在配有火焰离子化检测器和毛细管柱(HP-5, 30 m×0.32 mm×0.25 μm)的气相色谱(Agilent GC-7890B)上进行定量分析,以联苯为内标物。分析条件:载气为氮气,柱流速为1 mL·min<sup>-1</sup>,进样口和检测器温度均为280 °C,进样口分流比是50:1,柱箱程序升温,初始温度为60 °C,以10 °C·min<sup>-1</sup>的升温速率升至200 °C并保持4 min。转化率、选择性、转换频率(TOF)的计算公式:Conversion=(n<sub>0</sub>-n<sub>s</sub>)/n<sub>0</sub>×100%, Selectivity=n<sub>a</sub>/(n<sub>a</sub>+n<sub>b</sub>)×100%, TOF=n<sub>s</sub>/(n<sub>c</sub>t),其中n<sub>0</sub>为底物苄胺初始物质的量,n<sub>s</sub>为底物苄胺的物质的量,n<sub>a</sub>为产物亚胺的物质的量,n<sub>b</sub>为副产物的物质的量,n<sub>c</sub>为催化剂的物质的量,t为反应时间。所得产物经气相色谱-质谱联用仪(GC-MS, Agilent 7890N-5975)确认。

## 2 结果与讨论

### 2.1 催化剂表征

图2a为V-N-C和N-C的XRD图,在23.5°和43.0°处均出现2个明显的衍射峰,归属于无定型碳的(002)和(101)晶面<sup>[25-26]</sup>,说明V-N-C和N-C均属于部

分石墨化C基材料。此外,在图中并未发现V物种的特征衍射峰,说明催化剂中V物种分散度较高且颗粒尺寸较小。如图2b、2c所示,样品V-N-C、N-C的N<sub>2</sub>吸附量均较大,且均具有微孔/介孔复合结构,比表面积分别为1 470和1 000 m<sup>2</sup>·g<sup>-1</sup>,总的孔体积分别为1.06和0.54 cm<sup>3</sup>·g<sup>-1</sup>,较高的比表面积和多孔结构有助于反应物的吸附与扩散。通过ICP-AES测定V-N-C中金属V的质量分数为0.19%。如图2d所示,样品Raman光谱中均出现2个较强的峰,分别位于1 350 cm<sup>-1</sup>处的D带以及1 598 cm<sup>-1</sup>处的G带,I<sub>D</sub>/I<sub>G</sub>均为0.99,表明在高温碳化处理和酸漂洗后不仅使样品表面形成了一定量的石墨碳结构,同时也产生大量的缺陷<sup>[27-29]</sup>。图2e为V-N-C的高分辨率N1s XPS谱图,4个光电子峰分别归属于吡啶氮(398.3 eV)、吡咯氮(399.3 eV)、石墨氮(400.7 eV)和氧化氮(402.7 eV),表明经过高温碳化处理,壳聚糖分子中的N原子转化成不同的氮物种分布在碳骨架中。图2f为高分辨率V2p XPS谱图,其光电子峰很弱,说明样品中V含量相对较低,结果与XRD及ICP-AES相一致。由图3a可知,V-N-C样品呈现不规则块状结构,也没有出现明显的晶格条纹和V纳米颗粒(图3b、3c)。从图3d中观察到0.5 nm以下的孤立亮点(已用红圈标记)分散在多孔碳网中,因此我们推测V-N-C中V物种可能以单原子VN<sub>x</sub>形式高度分散在碳骨架中<sup>[30]</sup>。

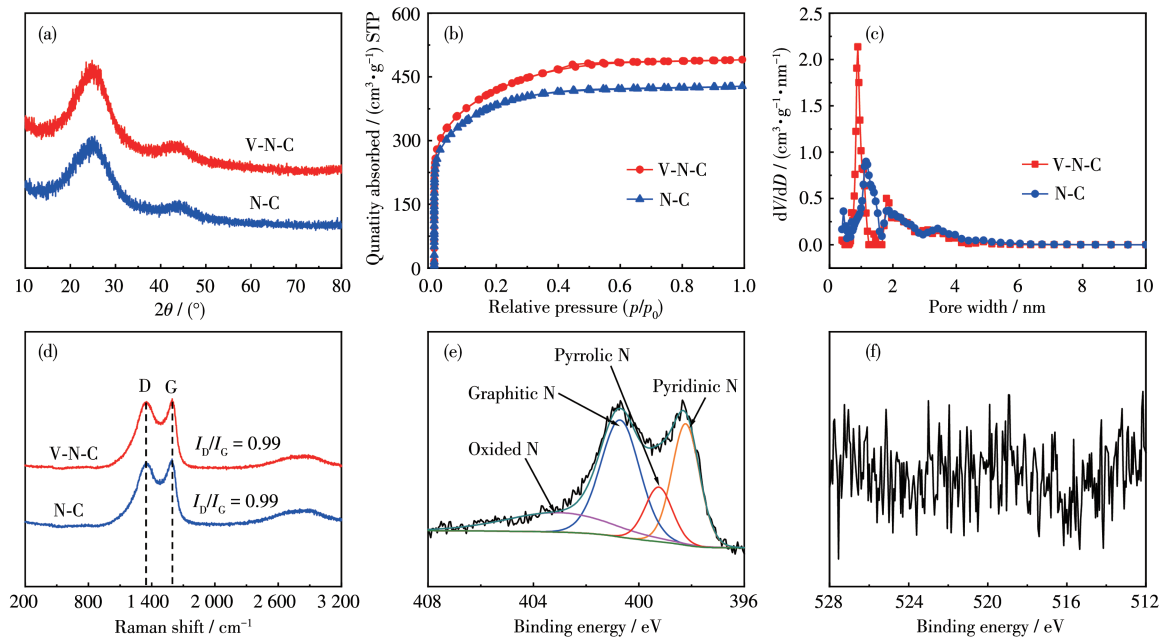


图2 V-N-C和N-C的(a)XRD图、(b)氮气吸附-脱附等温线、(c)孔径分布和(d)拉曼光谱图; V-N-C的(e)N1s和(f)V2p XPS谱图

Fig.2 (a) XRD patterns, (b)  $N_2$  adsorption-desorption isotherms, (c) pore size distributions, (d) Raman spectra of V-N-C and N-C; (e) N1s and (f) V2p XPS spectra of V-N-C

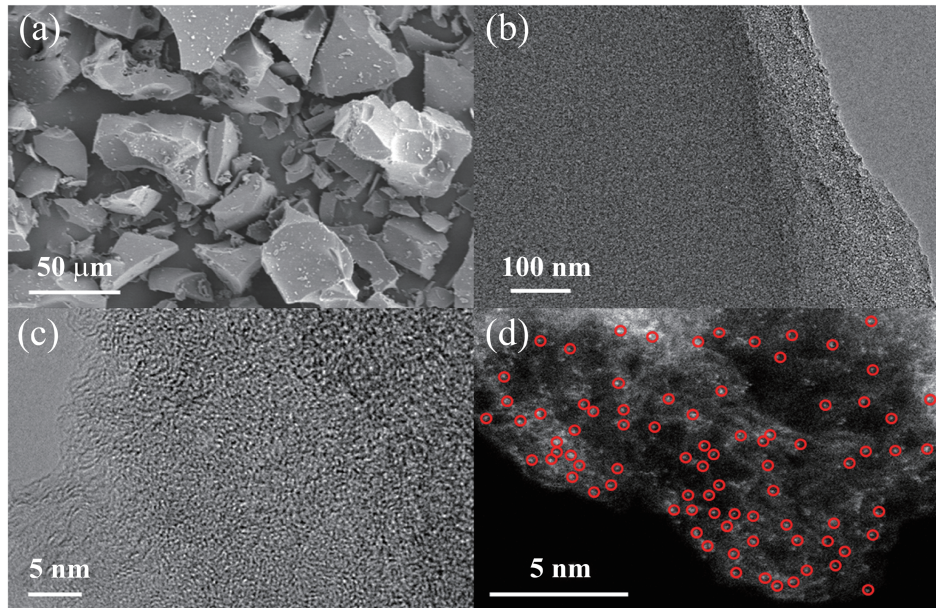


图3 V-N-C的(a)SEM图、(b)TEM图、(c)HRTEM图及(d)球差校正的HAADF-STEM图

Fig.3 (a) SEM image, (b) TEM image, (c) HRTEM image, (d) aberration-corrected HAADF-STEM image of V-N-C

## 2.2 催化剂反应性能

### 2.2.1 不同催化剂的催化效果

我们选择以 $O_2$ 为氧化剂的苯胺偶联反应作为探针反应,评价了V-N-C催化剂的催化性能。从表1中可见,在未加催化剂或只有载体N-C的情况下,几乎没有产物的生成(表1,Entry 2、5),说明V基催化剂在反应中不可或缺。与传统催化剂 $V_2O_5$ 和均

相催化剂 $VO(acac)_2$ 相比(Entry 3、4),V-N-C催化剂的氧化苯胺转化率高达99%,目标产物亚胺的选择性高达99%(Entry 1)。此外,我们还考察了V-N-C在无溶剂体系中的反应效果,通过适当延长反应时间,发现苯胺转化率仍可达94%,目标产物亚胺的选择性为99%(Entry 6)。以上结果说明呈单原子分散的V-N-C催化剂在苯胺氧化自偶联反应中具有非常高

的催化活性。而且,与已报道的催化剂(表2,Entry 1~5)相比,V-N-C催化剂展现出最高的TOF值,这可能与其高度分散的VN<sub>x</sub>中心有关,也进一步说明其具有优异的催化活性。

## 2.2.2 底物普适性

如表3所示,对V-N-C催化剂的底物适用范围进行了拓展。含有不同官能团的苄胺衍生物均能以较高的转化率和选择性转化为相应的亚胺(表3,Entry 1~9)。对于催化含杂原子胺的氧化偶联反应也具有较高的活性(Entry 10~12)。此外,也可以促进惰性脂肪胺(Entry 13)以及仲胺的氧化偶联(Entry 14)。

## 2.2.3 苄胺与不同胺的交叉偶联反应

我们也评价了V-N-C在苄胺与不同胺交叉偶联合成不对称亚胺反应中的催化效果。如表4所示,其转化率几乎都达100%,选择性也较高(表4,Entry 1~4)。此外,V-N-C在催化苄胺与环状或直链脂肪胺反应中的活性分别为81%和83%,目标产物的选择性分别为84%和73%(Entry 5、6)。评价结果进一步证明了V-N-C在胺-胺氧化偶联反应中具有良好的普适性。

## 2.2.4 热过滤实验和重复性能

如图4a所示,采用热过滤实验来判别V-N-C中活性组分的稳定性。当反应进行到90 min时通过

热过滤快速移除V-N-C催化剂,进一步延长反应时间,发现苄胺的转化率不再增加,稳定在49%左右,说明在使用过程中未出现任何活性V物种的溶脱问题,V-N-C催化剂上进行的氧化偶联反应是完全多相催化。另外,如图4b所示,考察了V-N-C的重复使用性,催化剂循环使用9次,催化性能没有任何下降,进一步说明V-N-C具有优良的重复性能。为了进一步验证回收催化剂的稳定性,对使用后的催化剂进行了XRD和HAADF-STEM分析(图5)。发现与新鲜催化剂对比,无论是材料结构还是钒物种尺寸,使用后的V-N-C均未发生明显变化,证实V-N-C催化剂在所考察的催化条件下具有良好的稳定性。

## 2.2.5 反应机理初探

结合实验结果和文献报道<sup>[35~37]</sup>,我们推测了V-N-C催化剂上苄胺合成亚胺的可能反应机理,如图6所示。在反应初期,苄胺在VN<sub>x</sub>位点活化转化为苄基亚胺**1b**<sup>[30]</sup>,氧气分子在缺陷位点活化形成中间物H<sub>2</sub>O<sub>2</sub><sup>[35]</sup>。此时,苄基亚胺**1b**可通过2条路径得到亚胺**1c**。路径A:**1b**与另一分子**1a**缩合脱去NH<sub>3</sub>,生成目标产物**1c**;路径B:**1b**与水作用生成苯甲醛,苯甲醛与另一分子**1a**缩合脱H<sub>2</sub>O生成目标产物**1c**。

我们采用比色法<sup>[4]</sup>验证反应中产生的中间体H<sub>2</sub>O<sub>2</sub>,由于H<sub>2</sub>O<sub>2</sub>可将过氧化物酶(POD)氧化,随后N,N-二乙基对苯二胺硫酸盐(DPD)被POD氧化为阳离

表1 不同催化剂在苄胺氧化自偶联中的催化性能

Table 1 Catalytic properties of various catalysts for oxidative self-coupling of benzylamine

Entry	Catalyst	Conversion / %	Selectivity / %	TOF / h <sup>-1</sup>
1 <sup>a</sup>	V-N-C	99	99	36.51
2 <sup>a</sup>	N-C	2	99	0
3 <sup>a</sup>	VO(acac) <sub>2</sub>	68	99	0.33
4 <sup>a</sup>	V <sub>2</sub> O <sub>5</sub>	45	99	0.06
5 <sup>a</sup>	—	1	99	0
6 <sup>b</sup>	V-N-C	94	99	389.85

<sup>a</sup> Reaction conditions: catalyst (30 mg), benzylamine (0.5 mmol), toluene (3 mL), O<sub>2</sub> pressure (1.01×10<sup>5</sup> Pa), 110 °C, 12 h; <sup>b</sup> Catalyst (60 mg), benzylamine (15 mmol), O<sub>2</sub> balloon (1.01×10<sup>5</sup> Pa), 110 °C, 16 h.

表2 不同催化剂上苄胺氧化自偶联反应活性比较

Table 2 Comparison of the oxidative self-coupling reaction activity of benzylamine over different catalysts

Entry	Catalyst	Time / h	Conversion / %	Selectivity / %	TOF / h <sup>-1</sup>	Ref.
1	V-N-C	12	99	99	36.51	This work
2	Co-N-C/SiO <sub>2</sub>	24	99	100	0.52	[31]
3	NHPI/Fe(BTC)	24	98	90	0.24	[32]
4	WOH-D nanosheets	2	69	99	0.85	[33]
5	Cu <sub>meth</sub> Al <sub>butox</sub>	15	99	99	0.36	[34]

表3 V-N-C催化多种胺生成亚胺的自偶联反应  
Table 3 Self-coupling reaction of various amines to imines catalyzed by V-N-C<sup>a</sup>

Entry	Substrate	Product	Conversion / %	Selectivity / %
1			99	100
2			98	99
3			99	99
4			99	99
5			91	93
6			98	98
7			96	98
8			96	99
9			88	84
10			94	97
11			99	91
12			98	99
13			60	67
14			92	98

<sup>a</sup>Reaction conditions: amine (0.5 mmol), V-N-C (30 mg), toluene (3 mL), O<sub>2</sub> pressure (1.01×10<sup>5</sup> Pa), 110 °C, 12 h.

表4 V-N-C催化1a与各种胺的交叉偶联反应

Table 4 Cross-coupling reaction of 1a with various amines catalyzed by V-N-C<sup>a</sup>

Entry	Amine 2	Conversion <sup>b</sup> / %	Selectivity <sup>b</sup> / %	
			4	3a
1		99	91	9
2		99	95	5
3		99	90	10
4		99	93	7
5		81	84	16
6		83	73	27

<sup>a</sup> Reaction conditions: **1a** (0.125 mmol), amine **2** (0.375 mmol), V-N-C (30 mg), toluene (3 mL), O<sub>2</sub> pressure (1.01×10<sup>5</sup> Pa), 110 °C, 12 h; <sup>b</sup> Conversion and selectivity were based on **1a** and confirmed by GC-MS.

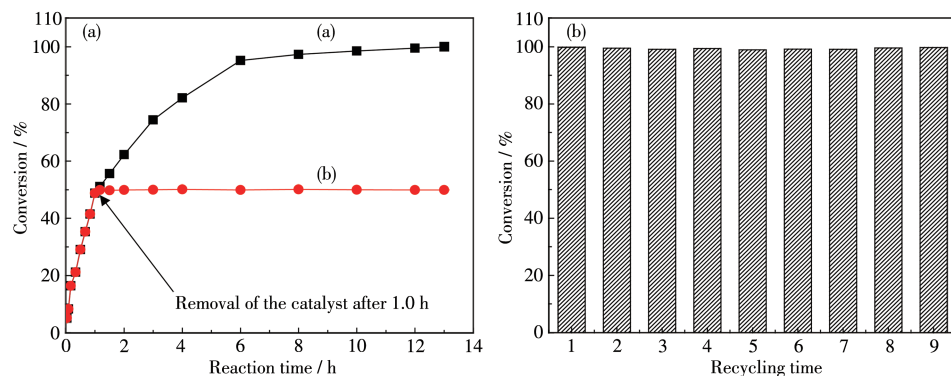


图4 V-N-C催化剂苄胺氧化自偶联中的(a)热过滤实验及(b)重复使用性

Fig.4 (a) Thermal filtration test and (b) reusability for the benzylamine oxidative self-coupling of V-N-C catalyst

子(DPD<sup>+</sup>)，DPD<sup>+</sup>在紫外可见(UV-Vis)吸收光谱中510和551 nm处显示2个吸收峰。结果如图7所示，随着反应时间延长，2个吸收峰的强度均明显增加，充

分说明苄胺氧化偶联过程中涉及到了H<sub>2</sub>O<sub>2</sub>。

为了验证苄基亚胺是反应的中间体，我们以N-亚苄基甲胺替代苄基亚胺，加入到V-N-C和苄胺中

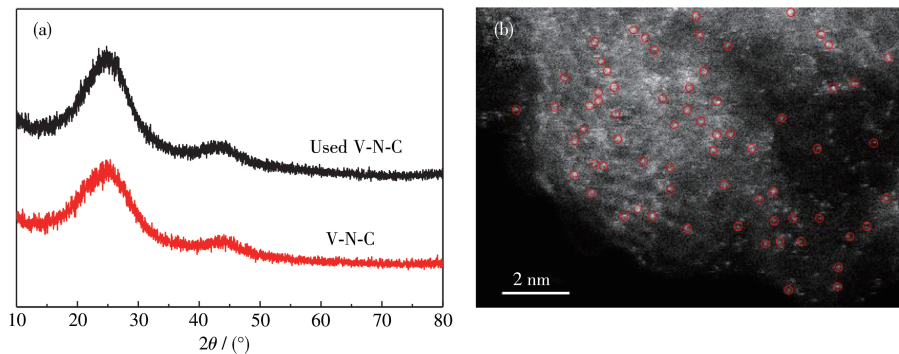


图5 使用后V-N-C催化剂(a) XRD图和(b)球差校正的HAADF-STEM图

Fig.5 (a) XRD pattern and (b) aberration-corrected HAADF-STEM image of spent V-N-C catalyst

进行反应,如图8所示,仅在1 h内就有74%的N-亚苄基甲胺转化为最终产物,进一步说明苄基亚胺是最可能的反应中间体。另外,由于在V-N-C催化苄胺氧化合成亚胺中未检测到任何醛类物质,基本排除了路径B的可能。

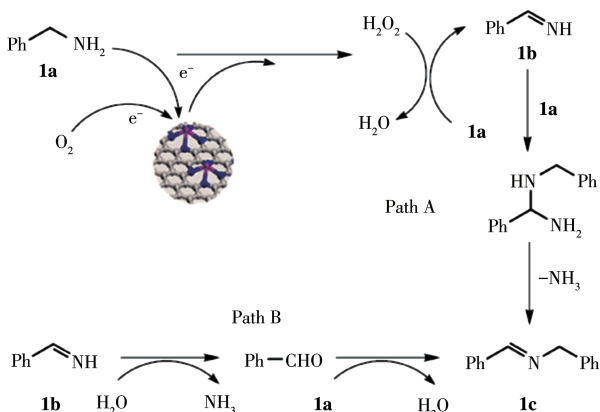


图6 V-N-C催化剂上苄胺合成亚胺可能反应机理

Fig.6 Possible reaction mechanism of benzylamine to imine catalyzed by V-N-C catalyst

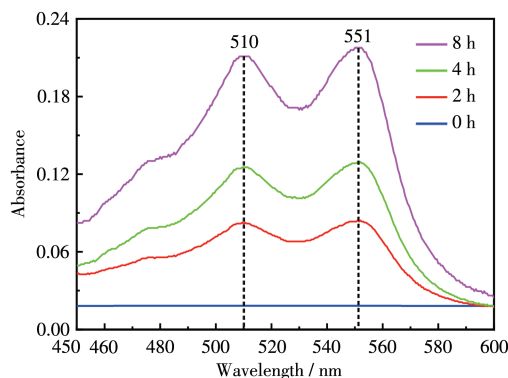
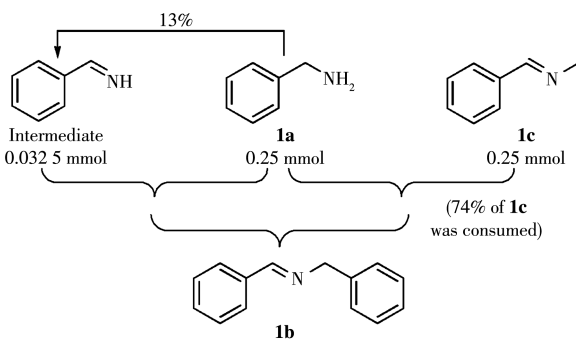
图7 V-N-C催化剂上DPD/POD试剂与H<sub>2</sub>O<sub>2</sub>反应后的UV-Vis吸收谱图Fig.7 UV-Vis absorption spectra of the DPD/POD reagent after reaction with H<sub>2</sub>O<sub>2</sub> over V-N-C

图8 苄胺和N-亚苄基甲胺在V-N-C催化剂上的氧化偶联反应

Fig.8 Oxidative coupling reaction of benzylamine and N-benzylidenemethyl amine over V-N-C catalyst

### 3 结论

以壳聚糖为前驱体,乙酰丙酮钒为金属源,氯化锌为造孔剂,采用简单的热处理结合酸洗的方法制备出一种高比表面积钒氮共掺杂多孔碳(V-N-C)催化剂,其在苄胺氧化偶联合成对称亚胺、交叉偶联合成不对称亚胺反应中均表现出优异的反应活性。这可能是由于V-N-C中V物种近乎以单原子形式高度分散在碳载体上,活性中心VN<sub>x</sub>充分暴露,使得其催化性能明显优于多相V<sub>2</sub>O<sub>5</sub>和均相VO(acac)<sub>2</sub>催化剂。此外,循环套用9次后,V-N-C的催化性能没有任何降低,说明其具有优良的稳定性,具有潜在应用前景。

### 参考文献:

- [1]Pahalagedara M N, Pahalagedara L R, Kriz D, Chen S Y, Beaulieu F, Thalgampitiya W, Suib S L. Copper Aluminum Mixed Oxide (CuAl MO) Catalyst: A Green Approach for the One - Pot Synthesis of Imines under Solvent-Free Conditions. *Appl. Catal. B*, **2016**, *188*:227-234

- [2] Dutta B, March S, Achola L, Sahoo S, He J K, Amin A S, Wu Y, Poges S, Alpay S P, Suib S L. Mesoporous Cobalt/Manganese Oxide: A Highly Selective Bifunctional Catalyst for Amine - Imine Transformations. *Green Chem.*, **2018**,*20*(14):3180-3185
- [3] Mohan D C, Sadhukha A, Maayan G. A Metallopeptoid as an Efficient Bioinspired Cooperative Catalyst for the Aerobic Oxidative Synthesis of Imines. *J. Catal.*, **2017**,*355*:139-144
- [4] Jin J J, Yang C J, Zhang B G, Deng K J. Selective Oxidation of Amines Using O<sub>2</sub> Catalyzed by Cobalt Thioporphyrazine under Visible Light. *J. Catal.*, **2018**,*361*:33-39
- [5] Gawronski J, Wascinska N, Gajewy J. Recent Progress in Lewis Base Activation and Control of Stereoselectivity in the Additions of Trimethylsilyl Nucleophiles. *Chem. Rev.*, **2008**,*108*(12):5227-5252
- [6] De S K, Gibbs R A. Bismuth Trichloride Catalyzed Synthesis of  $\alpha$ -Aminonitriles. *Tetrahedron Lett.*, **2004**,*45*(40):7407-7408
- [7] Das B, Laxminarayana K, Ravikanth B, Ramarao B. Efficient Synthesis of Homoallylic Alcohols and Amines Using 2,4,6-Trichloro-1,3,5-triazine. *Tetrahedron Lett.*, **2006**,*47*(51):9103-9106
- [8] Grirrane A, Corma A, Garcia H. Highly Active and Selective Gold Catalysts for the Aerobic Oxidative Condensation of Benzylamines to Imines and One-Pot, Two-Step Synthesis of Secondary Benzylamines. *J. Catal.*, **2009**,*264*(2):138-144
- [9] Liu P, Li C, Hensen E J M. Efficient Tandem Synthesis of Methyl Esters and Imines by Using Versatile Hydrotalcite - Supported Gold Nanoparticles. *Chem. Eur. J.*, **2012**,*18*(38):12122-12129
- [10] Mielby J, Poreddy R, Engelbrekt C, Kegnaes S. Highly Selective Formation of Imines Catalyzed by Silver Nanoparticles Supported on Alumina. *Chin. J. Catal.*, **2014**,*35*(5):670-676
- [11] Neeli C K P, Ganji S, Ganjala V S P, Kamaraju S R R, Burri D R. Oxidative Coupling of Primary Amines to Imines under Base-Free and Additive-Free Conditions over AuNPs/SBA-NH<sub>2</sub> Nanocatalyst. *RSC Adv.*, **2014**,*4*(27):14128-14135
- [12] Dai J, Yang J, Wang X H, Zhang L, Li Y J. Enhanced Visible-Light Photocatalytic Activity for Selective Oxidation of Amines into Imines over TiO<sub>2</sub>(B)/Anatase Mixed-Phase Nanowires. *Appl. Surf. Sci.*, **2015**,*349*:343-352
- [13] Sun D R, Ye L, Li Z H. Visible-Light-Assisted Aerobic Photocatalytic Oxidation of Amines to Imines over NH<sub>2</sub>-MiL-125(Ti). *Appl. Catal. B*, **2015**,*164*:428-432
- [14] Phasayavan W, Japa M, Pornsuwan S, Tantraviwat D, Kielar F, Golovko V B, Jungsuttiwong S, Inceesungvorn B. Oxygen-Deficient Bismuth Molybdate Nanocatalysts: Synergistic Effects in Boosting Photocatalytic Oxidative Coupling of Benzylamine and Mechanistic Insight. *J. Colloid Interface Sci.*, **2021**,*581*:719-728
- [15] Jin H H, Kou Z K, Cai W W, Zhou H, Ji P X, Liu B S, Radwan A, He D P, Mu S C. P—Fe Bond Oxygen Reduction Catalysts toward High-Efficiency Metal-Air Batteries and Fuel Cells. *J. Mater. Chem. A*, **2020**,*8*(18):9121-9127
- [16] Fu L L, Lu Y J, Liu Z G, Zhu R L. Influence of the Metal Sites of M-N-C (M=Co, Fe, Mn) Catalysts Derived from Metalloporphyrins in Ethylbenzene Oxidation. *Chin. J. Catal.*, **2016**,*37*(3):398-404
- [17] Zheng X J, Cao X C, Sun Z H, Zeng K, Yan J, Strasser P, Chen X, Sun S H, Yang R Z. Indiscrete Metal/Metal-N-C Synergic Active Sites for Efficient and Durable Oxygen Electrocatalysis toward Advanced Zn-Air Batteries. *Appl. Catal. B*, **2020**,*272*:118967
- [18] 徐凤勤, 胡小飞, 程方益, 梁静, 陶占良, 陈军. 多孔碳负载镍纳米颗粒的制备及催化氨硼烷水解制氢. *无机化学学报*, **2015**,*31*(1):103-108  
XU F Q, HU X F, CHENG F Y, LIANG J, TAO Z L, CHEN J. Preparation of Porous Carbon-Supported Ni Nanoparticles for Catalytic Hydrogen Generation from Ammonia Borane Hydrolysis. *Chinese J. Inorg. Chem.*, **2015**,*31*(1):103-108
- [19] Bisen O Y, Nandan R, Yadav A K, Pavithra B, Nanda K K. In Situ Self-Organization of Uniformly Dispersed Co-N-C Centers at Moderate Temperature without a Sacrificial Subsidiary Metal. *Green Chem.*, **2021**,*23*(8):3115-3126
- [20] Huang K X, Zhang W Q, Li J, Fan Y J, Yang B, Rong C Y, Qi J H, Chen W, Yang J. In Situ Anchoring of Zeolite Imidazole Framework-Derived Co, N-Doped Porous Carbon on Multiwalled Carbon Nanotubes toward Efficient Electrocatalytic Oxygen Reduction. *ACS Sustainable Chem. Eng.*, **2020**,*8*(1):478-485
- [21] Sun J T, Niu J, Liu M Y, Ji J, Dou M L, Wang F. Biomass-Derived Nitrogen-Doped Porous Carbons with Tailored Hierarchical Porosity and High Specific Surface Area for High Energy and Power Density Supercapacitors. *Appl. Surf. Sci.*, **2018**,*427*:807-813
- [22] Sun L, Fu Y, Tian C G, Yang Y, Wang L, Yin J, Ma J, Wang R H, Fu H G. Isolated Boron and Nitrogen Sites on Porous Graphitic Carbon Synthesized from Nitrogen-Containing Chitosan for Supercapacitors. *ChemSusChem*, **2014**,*7*(6):1637-1646
- [23] Yang Y H, Cui J H, Zheng M T, Hu C F, Tan S Z, Xiao Y, Yang Q, Liu Y L. One-Step Synthesis of Amino-Functionalized Fluorescent Carbon Nanoparticles by Hydrothermal Carbonization of Chitosan. *Chem. Commun.*, **2012**,*48*(3):380-382
- [24] Yu Z L, Li G C, Fechler N, Yang N, Ma Z Y, Wang X, Antonietti M, Yu S H. Polymerization under Hypersaline Conditions: A Robust Route to Phenolic Polymer-Derived Carbon Aerogels. *Angew. Chem. Int. Ed.*, **2016**,*55*(47):14623-14627
- [25] Liu W G, Zhang L L, Liu X, Liu X Y, Yang X F, Miao S, Wang W T, Wang A Q, Zhang T. Discriminating Catalytically Active FeN<sub>x</sub> Species of Atomically Dispersed Fe-N-C Catalyst for Selective Oxidation of the C—H Bond. *J. Am. Chem. Soc.*, **2017**,*139*(31):10790-10798
- [26] Qi Y Y, Xu Q H, Tu G M, Fu Y H, Zhang F M, Zhu W D. Vanadium Oxides Anchored on Nitrogen-Incorporated Carbon: An Efficient Heterogeneous Catalyst for the Selective Oxidation of Sulfide to Sulfoxide. *Catal. Commun.*, **2020**,*145*:106101
- [27] Wang X X, Cullen D A, Pan Y T, Hwang S, Wang M Y, Feng Z X, Wang J Y, Engelhard M H, Zhang H G, He Y H, Shao Y Y, Su D, More K L, Spendelow J S, Wu G. Nitrogen-Coordinated Single Cobalt Atom Catalysts for Oxygen Reduction in Proton Exchange Membrane Fuel Cells. *Adv. Mater.*, **2018**,*30*(11):1706758
- [28] Yin P Q, Yao T, Wu Y, Zheng L R, Lin Y, Liu W, Ju H X, Zhu J F, Hong X, Deng Z X, Zhou G, Wei S Q, Li Y D. Single Cobalt Atoms with Precise N-Coordination as Superior Oxygen Reduction Reaction

- Catalysts. *Angew. Chem. Int. Ed.*, **2016**, *55*(36):10800-10805
- [29] 吴晓敏, 毛剑, 周志鹏, 张臣, 卜静婷, 李珍. 氮掺杂石墨烯量子点/MOF衍生多孔碳纳米片构筑高性能超级电容器. 无机化学学报, **2020**, *36*(7):1298-1308
- WU X M, MAO J, ZHOU Z P, ZHANG C, BU J T, LI Z. Building a High-Performance Supercapacitor with Nitrogen-Doped Graphene Quantum Dots/MOF-Derived Porous Carbon Nanosheets. *Chinese J. Inorg. Chem.*, **2020**, *36*(7):1298-1308
- [30] Xu Q H, Feng B B, Ye C L, Fu Y H, Chen D L, Zhang F M, Zhang J W, Zhu W D. Atomically Dispersed Vanadium Sites Anchored on N-Doped Porous Carbon for the Efficient Oxidative Coupling of Amines to Imines. *ACS Appl. Mater. Interfaces*, **2021**, *13*(13):15168-15177
- [31] Zhang C H, Zhao P S, Zhang Z L, Zhang J W, Yang P, Gao P, Gao J, Liu D. Co-N-C Supported on SiO<sub>2</sub>: A Facile, Efficient Catalyst for Aerobic Oxidation of Amines to Imines. *RSC Adv.*, **2017**, *7*(75):47366-47372
- [32] Dhakshinamoorthy A, Alvaro M, Garcia H. Aerobic Oxidation of Benzyl Amines to Benzyl Imines Catalyzed by Metal-Organic Framework Solids. *ChemCatChem*, **2010**, *2*(11):1438-1443
- [33] Zhang N, Li X Y, Liu Y F, Long R, Li M Q, Chen S M, Qi Z M, Wang C M, Song L, Jiang J, Xiong Y J. Defective Tungsten Oxide Hydrate Nanosheets for Boosting Aerobic Coupling of Amines: Synergistic Catalysis by Oxygen Vacancies and Brønsted Acid Sites. *Small*, **2017**, *13*(31):1701354
- [34] Dissanayake D, Achola L A, Kerns P, Rathnayake D, He J, Macharia J, Suib S L. Aerobic Oxidative Coupling of Amines to Imines by Mesoporous Copper Aluminum Mixed Metal Oxides via Generation of Reactive Oxygen Species (Ros). *Appl. Catal. B*, **2019**, *249*:32-41
- [35] Chen B, Wang L Y, Dai W, Shang S S, Lv Y, Gao S. Metal-Free and Solvent-Free Oxidative Coupling of Amines to Imines with Mesoporous Carbon from Macrocyclic Compounds. *ACS Catal.*, **2015**, *5*(5):2788-2794
- [36] Zhang N, Li X Y, Liu Y F, Long R, Li M Q, Chen S M, Qi Z M, Wang C M, Song L, Jiang J, Xiong Y J. Defective Tungsten Oxide Hydrate Nanosheets for Boosting Aerobic Coupling of Amines: Synergistic Catalysis by Oxygen Vacancies and Bronsted Acid Sites. *Small*, **2017**, *13*(31):1701354
- [37] Qiu X, Len C, Luque R, Li Y W. Solventless Oxidative Coupling of Amines to Imines by Using Transition-Metal-Free Metal-Organic Frameworks. *ChemSusChem*, **2014**, *7*(6):1684-1688